

PRE-EQUILIBRIUM PLASMA DYNAMICS^{*1}

Ulrich HEINZ

Physics Department, Brookhaven National Laboratory, Upton, NY 11973, USA

Approaches towards understanding and describing the pre-equilibrium stage of quark-gluon plasma formation in heavy-ion collisions are reviewed.

1. INTRODUCTION

The concept of local thermal and chemical equilibrium in heavy-ion collisions is very useful for both theorists and experimentalists because it drastically economizes the description of the collision process and the interpretation of data. Theoretically, it fixes the local momentum distribution of the particles in terms of usually two parameters, the local temperature T and the local baryon chemical potential μ , which are completely determined by specifying the local energy and baryon density. It allows a unique separation of intrinsic thermal motion and the collective flow, and leads to a hydrodynamical description of the space-time evolution in terms of the densities and the local flow vector only, rather than in terms of the full phase-space distribution of the particles. Experimentally, a comparison of particle spectra with thermal distributions provides an intuitive feeling for the "violence" of the collision in terms of the easily grasped notions of "temperature" and "compression."

Much of our present understanding of the expected life history of a quark-gluon plasma in nuclear collisions, its decay back into hadrons, and the traces it leaves behind, is based on such a thermal description. Still, it is clear from a principal point of view that local equilibrium cannot be achieved instantaneously in these collisions. Due to the relativistic beam energies, many particles will be produced, in particular if the nucleons and mesons indeed dissolve into a giant quark soup, and their initial distribution cannot be expected to be thermal. As shown in Fig. 1, the (hopefully locally equilibrated) quark-gluon plasma, mixed (for a first order hadronization transition), and hadronic gas phases will be preceded by a pre-equilibrium stage, in which additional particles are created and scatter with each other towards equilibrium.

*1) This work was supported by the U. S. Department of Energy under Contract DE-AC02-76CH00016.

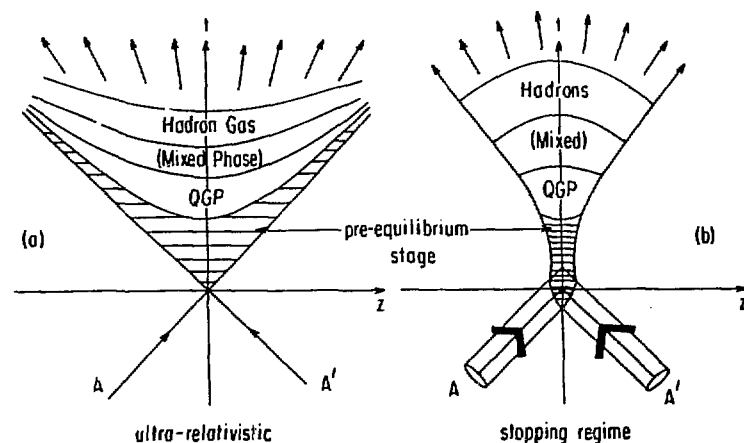


Figure 1. Artist's view, looked at from the center of mass, of the expected space-time scenarios in (a) ultrarelativistic ("transparent") nuclear collisions ($E_{CM} > 100 \text{ GeV/nucleon}$) and (b) in the stopping regime ($E_{CM} < 5 \text{ GeV/nucleon}$). In zeroth approximation, i.e. neglecting transverse flow in (a) and side-splash-effects in (b), Fig. 1a is unchanged as one moves into the transverse direction, and Fig. 1b is rotationally symmetric around the t -axis.

In the Figure it is (optimistically) assumed that the pre-equilibrium phase, dominated by particle formation and collisions/equilibration, has a shorter time scale than the lifetime of the hot fireball before it decouples into free-streaming particles, and in particular shorter than the plasma phase lifetime. Hydrodynamic simulations of the expanding plasma^{1,2} in ultra-relativistic collisions show that even for initial temperatures (energy densities) far above the critical values the lifetime of the quark-gluon plasma phase never exceeds about 10 fm/c . On the other hand, simple kinetic models³ predict that the energy density does not behave hydrodynamically, i.e., thermalization is not completed for the average momenta, before $\tau \sim 10 \tau_c$ where τ_c is the mean collision time (see Fig. 5). Therefore, unless τ_c is very much smaller than the typical strong interaction time scale of 1 fm/c , thermalization of the quark-gluon plasma before the beginning of hadronization is doubtful. Even if local equilibrium is reached by then, the large change in energy and entropy density across the phase transition region will almost certainly destroy at least chemical equilibrium⁴, never to be reestablished before freezeout. The strangeness⁵ and antibaryon⁴ signals for quark matter formation partially rely on this feature.

A number of theoretical concepts for a non-equilibrium dynamical description of nuclear collisions without assuming local equilibrium have been developed in the recent years and were put to practical use in simulating collisions at Bevalac energies (100 MeV/nucleon to 1 GeV/nucleon). For a comprehensive overview and references, see the review by Stöcker and Greiner⁶ and the talk by Aichelin at the Santa Fe meeting⁷. All these approaches work with hadronic degrees of freedom; a transition to quark-gluon matter has not been implemented. In the

- Classical Cascade Model the nucleons are assumed to move as classical particles on straight lines (the nuclear mean field and long-range two-body interactions are neglected), until they collide elastically or inelastically according to the free nucleon-nucleon cross-section. Pauli-blocking on the scattered nucleons is usually neglected or taken into account in a simplified way.
- Classical Molecular Dynamics includes long-range two-body interactions $V(r)$, and the particles move on curved trajectories which are solutions of the Newtonian equations of motion. In this approach inelastic nucleon collisions and particle production are neglected. The same applies to
- Quantum Molecular Dynamics, where, however, the classical particles are replaced by quantum wavepackets when the mean field potential governing their trajectories is computed. This permits rewriting the mean field in terms of density dependent interactions and provides a connection to the nuclear equation of state $E(\rho)$. The advantage of the molecular dynamics approach is that it allows studying fluctuations and clustering, leading to fragmentation as in a real collision.

If one does not wish to work with wavepackets, the connection to the nuclear matter equation of state is possible, if instead of a single classical molecular dynamics run one performs many simultaneous runs in which all the particles are moving in a common mean field whose density dependence is determined by statistically averaging over the particle positions in all the different runs at a given timestep. In this procedure, however, one loses information about fluctuations, and one essentially simulates the evolution of a phase-space distribution function $f(\vec{x}, \vec{v}, t)$ according to the Vlasov equation. Adding random (inelastic) scattering using the free nucleon-nucleon cross-section with Pauli-blocking on the final states, a collision term is effectively included into this kinetic equation. This approach has been dubbed "Vlasov-Uehling-Uhlenbeck (VUU)" simulation, although the name Vlasov-Boltzmann-Nordheim⁸ equation is historically more appropriate.

- Hydrodynamics is recovered from this equation by taking low-order moments in momentum space and inserting the local equilibrium Bose-Einstein or Fermi-Dirac distributions for the phase-space distribution functions.

In my talk I will focus on this kinetic theory approach to non-equilibrium dynamics, its extension to include the dynamics of color degrees of freedom when applied to the quark-gluon plasma, its quantum field theoretical foundations, and its relationship to both the particle formation stage at the very beginning of the nuclear collision and the hydrodynamic stage at late collision times. I will discuss its usefulness to obtain the transport coefficients in the quark-gluon plasma and to derive the collective mode spectrum and damping rates in this phase. I will comment on the general difficulty to find appropriate initial conditions to get the kinetic theory started, but also show a specific model which demonstrates that, once given such initial conditions, we actually can follow the system all the way through into the hydrodynamical regime. In other words, we are at the verge of being able to compute plasma signatures like, say, lepton-pair spectra with non-equilibrium quark and gluon distribution functions as an input⁹.

2. A SHORT INTRODUCTION TO KINETIC THEORY

2.1 Classical Kinetic Theory

The object of kinetic theory is the phase-space distribution function $f(\vec{x}, \vec{p}, t)$ or, in covariant notation, $f(x, p)$ with 4-vectors x^μ and p^ν . Classically, $f(x, p)$ is only non-vanishing on mass-shell, $p_0 = \sqrt{p^2 + m^2}$, a condition ensured by a δ -function $\delta(p^2 - m^2)$ in the Lorentz invariant momentum space integration measure. The equation of motion for $f(x, p)$ (kinetic equation) will drive the distribution function towards its local equilibrium form:

$$f_{eq}(x, p) = 1 / \{ \exp[\beta(x) \{ p^\mu u_\mu(x) - \mu(x) \}] \pm 1 \} . \quad (1)$$

Here $\beta(x)$ is the inverse local temperature, $\mu(x)$ the local chemical potential, $u_\mu(x)$ the 4-vector describing the average local flow of matter, and the upper (lower) sign is for bosons (fermions). In the local rest frame (where $u(x)=0$) eq. (1) reduces to the well-known Bose-Einstein (Fermi-Dirac) distributions.

Non-relativistically the kinetic equation takes the form

$$\frac{df}{dt} \equiv \frac{\partial f}{\partial t} + \frac{d\vec{x}}{dt} \cdot \vec{\nabla} f + \frac{d\vec{p}}{dt} \cdot \vec{\nabla}_p f = - \left(\frac{\partial f}{\partial t} \right)_{coll} , \quad (2)$$

with $\{\partial f / \partial t\}_{coll}$ describing the two-body collisions. The left-hand side describes the change in $f(\vec{x}, \vec{p}, t)$ due to phase-space flow. Substituting for

\dot{dp}/dt the Newtonian force in terms of the gradient of a mean field potential $-\vec{\nabla}U(\mathbf{r})$ brings the left hand side into the typical form of a Vlasov-equation. Assuming for the collision term the form invented by Boltzmann and Nordheim, eq. (2) finally reads

$$\frac{\partial f}{\partial t} + \vec{v} \cdot \vec{\nabla} f - \vec{\nabla} U \cdot \vec{\nabla}_p f = - \int d\vec{p}_1 d\vec{p}_2 \delta(\vec{p}_1 + \vec{p}_2 - \vec{p}) [f_1 f_2 (1 \pm f) - f_1' f_2' (1 \pm f')] \cdot \quad (3)$$

The main physical ingredients are the two-body cross section σ and the mean field $\vec{\nabla}U$, to be selfconsistently calculated from, say, a Poisson equation $\Delta U = 4\pi\rho = \int f d\vec{p}/2\pi^2$. Extracting from the right hand side of eq. (3) those distribution functions which are not integrated over, the collision term takes the form of a master equation

$$- \left(\frac{\partial f}{\partial t} \right)_{\text{coll}} = - f \Gamma_{\text{loss}} + (1 \pm f) \Gamma_{\text{gain}} \cdot \quad (4)$$

The factor $(1 \pm f)$ in front of the gain term accounts for the Pauli suppression (Bose enhancement) if the cell (\mathbf{x}, \mathbf{p}) is already occupied. The gain and loss rates Γ_{gain} , Γ_{loss} are, of course, space and momentum dependent. In local equilibrium the collision term vanishes, such that there

$$\frac{\Gamma_{\text{gain}}(\mathbf{x}, \mathbf{p})}{\Gamma_{\text{loss}}(\mathbf{x}, \mathbf{p}) \mp \Gamma_{\text{gain}}(\mathbf{x}, \mathbf{p})} = f_{\text{eq}}(\mathbf{x}, \mathbf{p}) \cdot \quad (5)$$

Defining an energy dependent equilibration rate

$$\Gamma \equiv \Gamma_{\text{loss}} \mp \Gamma_{\text{gain}} \equiv 1/\tau_0 \cdot \quad (6)$$

the collision term near equilibrium takes on the relaxation time form

$$\frac{\partial f}{\partial t} + \vec{v} \cdot \vec{\nabla} f - \vec{\nabla} U \cdot \vec{\nabla}_p f = -(f - f_{\text{eq}})/\tau_0 \cdot \quad (7)$$

In relativistic notation (multiply through by E/m) we get

$$\frac{df}{dt} \equiv \dot{x}_\mu \partial^\mu f + \dot{p}_\mu \partial_p^\mu f = - p \cdot u(\mathbf{x}) (f - f_{\text{eq}})/(m\tau_0) \cdot \quad (8)$$

Now the only remaining step is to substitute the relativistic equations of motion $m\dot{x}^\mu = p^\mu$ and, say, for a charged particle in an electromagnetic field the Lorentz force law $m\dot{p}^\mu = e F^{\mu\nu} p_\nu$, and we have the relativistic kinetic equation for an electron plasma:

$$p^\mu \partial_\mu f + e F_{\mu\nu}(x) p^\mu \partial_p^\nu f = - p \cdot u(x) (f - f_{\text{eq}}(x))/\tau_0 \cdot \quad (9)$$

The mean electromagnetic field is determined by (dP denotes the momentum space integration measure)

$$\partial_\mu F^{\mu\nu}(x) = e j^\nu(x) = e \int p^\nu f(x, p) dP \cdot \quad (10)$$

If we want to apply this formalism, in particular eqs. (9,10), to the quark-gluon plasma, a slight complication occurs: the color charge on the quarks and gluons is not a constant; it changes with every interaction with the mean color field which carries color itself and can exchange it with the particles.

Therefore, the color charge has to be considered as a dynamical variable like the particle momentum. Describing the eight coupling strengths of the particle to the eight color components of $F_{\mu\nu}$ by an 8-dimensional vector $\vec{g}Q$ (g is the strong coupling constant), the colored particle distribution function $f(\mathbf{x}, \mathbf{p}, \vec{Q})$ now lives in a larger color phase space, and eq. (8) has to be amended by a term $Q_a \partial_a f$ on the left hand side. Substituting the classical equation of motion¹⁰ for \vec{Q} in the mean color field $F_{\mu\nu}^a(x)$, and generalizing the Lorentz force law for \vec{p}_μ , we obtain¹¹ instead of eq. (9)

$$p^\mu (\partial_\mu - g Q_a F_{\mu\nu}^a(x) \partial_p^\nu - g f_{abc} A_\mu^b(x) Q^c \partial_Q^a) f = - p \cdot u(x) (f - f_{\text{eq}})/\tau_0 \cdot \quad (11)$$

The equation for the distribution function \bar{f} of antiparticles (which in the QCD plasma are as important as the particles) is analogous, except for a sign change in the second term, due to the opposite sign in color charge. The self-consistency equation is now the Yang-Mills equation,

$$\partial_\mu F_a^{\mu\nu}(x) + g f_{abc} A_\mu^b(x) F_c^{\mu\nu}(x) = g j_a^\nu(x) = g \int Q_a p^\nu (f - \bar{f}) dP dQ \cdot \quad (12)$$

where dQ is the integration measure in color space and contains two δ -functions $\delta(Q^2 - q_0^2) \delta(d_{abc} Q^a Q^b Q^c - q_1^3)$ fixing the Casimir invariants of the color representation of the colored particles¹¹. (This is analogous to the mass-shell δ -function in momentum space.)

2.2 Quantum Kinetic Theory

The quantum analogue of the phase space distribution function is the Wigner function or expectation value of the Wigner operator, which for quarks is defined by

$$\hat{F}(\mathbf{x}, \mathbf{p}) = - \int \frac{d^4 y}{(2\pi)^4} e^{-ip \cdot y} e^{-iy \cdot D_x/2} \psi(x) \bar{\psi}(x) e^{y \cdot D_x^\dagger/2} \cdot \quad (13)$$

The appearance of the covariant derivative $D_x = \partial/\partial x - i(g/2)[\lambda_a A^a, \cdot]$ (its adjoint D_x^\dagger acts to the left) makes this expression gauge invariant and, through Weyl's correspondence principle (see, e.g., Ref. 12), tells us that the argument p of \hat{F} is the kinetic (rather than the canonical) momentum $p^\mu = m\dot{x}^\mu$ (as

it should be, at least in the classical limit). The gauge invariance is most easily proven by using the identity¹³

$$e^{-y \cdot D_x / 2} \psi(x) = P \exp(i \frac{g}{2} \lambda_a \int_{x-y/2}^x A_{\mu}^a(z) dz^{\mu}) \psi(x-y/2) \quad (14)$$

where the path from $x-y/2$ to x in the path ordered product is a straight line. Inserting (14) and its adjoint into (13) leads to the form for \hat{F} given some time ago¹⁴ while at the same time specifying the path to be linear. The gauge invariance of \hat{F} then relies on the known gauge transformation properties of the path ordered exponentials¹⁴.

Using the Dirac equation for the quark field operators, an exact equation of motion for \hat{F} was derived in Ref. 13. The result is very lengthy, and its complete interpretation will require much more work. However, a semiclassical expansion, keeping only the lowest order terms in momentum derivatives of \hat{F} and commutators of \hat{F} with the gluon field operators $A_{\mu}^a \lambda_a$, can be performed, and one obtains

$$p^{\mu} D_{\mu} \hat{F}(x,p) + \frac{g}{4} p^{\mu} \partial_{\nu} \{ F_{\mu\nu}^a \lambda_a, \hat{F}(x,p) \} + \frac{ig}{8} (\sigma^{\mu\nu} F_{\mu\nu}^a \lambda_a, \hat{F}(x,p)) = \hat{C}(x,p). \quad (15)$$

The "collision term" $\hat{C}(x,p)$ contains all higher order terms. Except for the spin term $\sim \sigma^{\mu\nu}$, this was already derived three years ago, and it was shown¹⁴ by decomposing (15) into its color and positive and negative frequency (particle and antiparticle) components that the two lowest color moments of the classical equations (11) are exactly recovered. Higher order color moments in the quantum case are redundant and can be reduced to the singlet and octet moments by using the color algebra; this information is lost at the purely classical level, but easily implemented a posteriori by appropriately truncating the color hierarchy¹¹.

Whereas the classical kinetic theory for colored quarks can be said to stand on solid quantum mechanical foundations, the quantum kinetic theory for gluons has not yet been found. The problem lies in the nature of the gluons as gauge particles and in their self-interaction, which makes the definition of a quantum distribution function for gluons with the correct gauge transformation properties a non-trivial task. Still, whatever the quantum kinetic equation will turn out to be, it will have to reduce to eq. (11) (or its color moments) in the classical limit.

While the semiclassical expansion leading to eq. (15) is essentially an expansion in powers of \hbar , it is coupled with an expansion in the strong coupling constant g through the covariant derivative. Thus, its range of

validity is, to some extent, governed by the smallness of g . In conventional nuclear physics, we don't have such a small expansion parameter, and alternative expansion schemes for the quantum kinetic theory are required. A new truncation scheme based on expanding the Wigner function into moments of the momentum operator was recently proposed in Ref. 15.

3. THE HYDRODYNAMIC CONNECTION

3.1 Chromo-hydrodynamics

Using energy-momentum, baryon number, and color conservation by the two-body collision term in the kinetic equation, it is straightforward¹¹ to derive macroscopic conservation laws for the baryon number current,

$$b_{\mu}(x) = \sum_{f,s} \int p^{\mu} (f - \bar{f}) d^3p dQ, \quad (16a)$$

the color current,

$$j_a^{\mu}(x) = \sum_s \int p^{\mu} Q_a \left(\int_f (f - \bar{f}) + g \right) d^3p dQ, \quad (16b)$$

and the energy momentum tensor,

$$T^{\mu\nu}(x) = \sum_s \int p^{\mu} p^{\nu} \left(\int_f (f - \bar{f}) + g \right) d^3p dQ, \quad (16c)$$

by multiplying eq. (11) with the appropriate factors of p^{μ} and Q_a and integrating over momentum and color space. In (16) we have included the gluon contribution via a (classical) gluon distribution function $g(x,p,Q)$ (which solves an equation exactly like eq. (11)), and the sums go over quark flavors and quark and gluon spin directions. The conservation laws read¹¹

$$\partial_{\mu} b^{\mu} = 0, \quad (17a)$$

$$\partial_{\mu} j_a^{\mu} + g f_{abc} A_{\mu}^b j_c^{\mu} = 0, \quad (17b)$$

$$\partial_{\mu} T^{\mu\nu} - g j_a^{\mu} \partial_{\mu} A^{\nu a} = 0, \quad (17c)$$

where again A_{μ}^b , $F_c^{\mu\nu}$ are the color mean fields in the systems. The second terms in (17a,b,c) are the divergences of the color current and energy-momentum carried by that mean field, so that in each case the sum of contributions from the particles (eqs. (16)) and from the mean field is conserved, i.e. color and energy-momentum can be exchanged between particles and field, but is not lost.

Inserting the local equilibrium form (1) for the distribution functions into the moments (16), one finds the following decomposition in terms of the local flow vector $u_{\mu}(x)$:

with different proportionality constants for the different channels. Inserting this into the expression for η , using a running value for α_s parametrized by the QCD mass scale Λ , Danielewicz and Gyulassy¹⁶ studied the effect of shear viscosity on a longitudinally hydrodynamically expanding plasma.

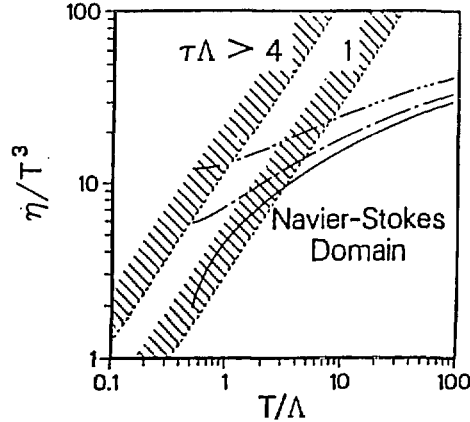


Figure 2. (From Ref. 16) The shear viscosity η as a function of temperature. The shaded regions indicate for which range of temperatures the corrections to longitudinal hydrodynamic expansion invalidate the Navier-Stokes approximation at early times ($\tau\Lambda=1$) and at later times ($\tau\Lambda=4$), respectively.

As shown in Figure 2, unless the initial temperature is very high or one restricts the (viscous) hydrodynamic description only to the later stages of the expansion, the corrections to hydrodynamic flow from viscosity effects are so large that the near-equilibrium expansion (19) does not make sense. In the space-time region indicated by the shaded areas in Fig. 2, one has to resort to a completely kinetic description.

Finally, the color conductivity tensor $\sigma_{ab}^{\mu\nu}$ was computed in Ref. 19. It is diagonal in color and (in the local rest frame) in the space time indices:

$$\sigma_{ab}^{\mu\nu} = \delta_{ab} (g^{\mu\nu} - u^\mu u^\nu) \tau_0 \Omega_p^2, \quad (24)$$

with the plasma frequency Ω_p given by

$$\Omega_p^2 = \frac{4\pi}{3} \alpha_s T^2 \left(1 + \frac{1}{6} \sum_f (1 + 3(\mu_f/\pi T)^2) \right). \quad (25)$$

However, in this case τ_0 is not dominated by quark-quark and quark-gluon scattering, but by pair creation processes. This will be discussed below in Section 5, where we look at the damping rate for color perturbations. To our

surprise we will find a negative value of τ_0 , indicating instability of the color neutral equilibrium state and a tendency of the system to move towards a new ground state in which local color structures are present.

4. FAR OFF-EQUILIBRIUM SITUATIONS AND INITIAL CONDITIONS

In this section I borrow heavily from the talk by Rudi Hwa presented at the Santa Fe meeting last week²⁰. He pointed out that there are essentially two models for the primordial quark and gluon distribution in the literature, which might become input candidates into a kinetic framework. In the

• String Model which was invented in connection with hadron production in e^+e^- annihilation, the primary $q\bar{q}$ pair, while separating with the velocity of light,

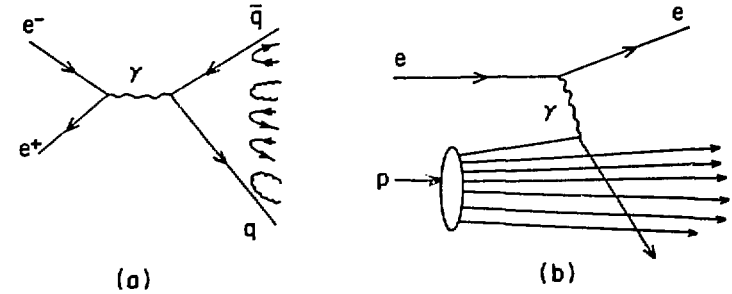


Figure 3. Quark and gluon production in the string model (a) and the parton model (b), schematically.

forms a string of color electric field (Fig. 4a), which then decays into hadrons by producing additional $q\bar{q}$ and gluon pairs in the electric field from the vacuum (Fig. 3a). In the

• Parton Model, successful in the description of deep inelastic ep collisions

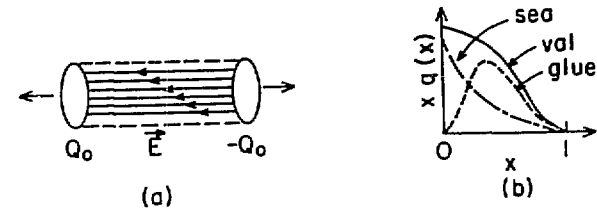


Figure 4. (a) Color string formed in pp collisions; \vec{E} denotes the color electric field, Q_0 the charge at the end of the string. (b) Schematic picture of the x -distribution of partons inside a proton.

(see Fig. 3b), all the quarks and gluons are present inside the proton from the beginning (although off-shell), described by distribution functions $F(x, Q^2)$, (Fig. 4b), and only have to be brought on-shell in the collision.

Both of these models have been applied to $p\bar{p}$ collisions, but with only partial success. In both cases there were in particular problems with the shape of the hadronic multiplicity distributions. A fundamental uncertainty of the string model in $p\bar{p}$ and, even more so, in $A + A$ collisions is the color charge Q_0 one should put on the ends of the string (Fig. 4a). Furthermore, nucleons contain sea quarks which can scatter and contribute further strings to the collision process. In the parton model the non-trivial soft interactions between partons may lead to cluster formation, thereby complicating the picture. In any case, neither of these models gives a clear prediction for the initial phase-space distribution of the quarks and gluons produced in nuclear collisions, and even the space-time history of particle production is not clear. Much work is necessary before we will know definitely how to begin the thermalization process, e.g. by using kinetic theory.

So far, two toy models have been played through. Rwa and Kajantie²¹ put the partons inside the nucleons (with their experimentally known x -distributions) on mass-shell by hand and made direct contact with thermodynamics by fitting the resulting τ -dependent parton and energy densities with thermal distributions. By this approach they circumvented the need for kinetic theory. The time at which the fit was performed was determined by equating the time-dependent ratio $\epsilon'/\rho' = f(\tau)$ for the free-streaming partons with the thermodynamic relation $\epsilon/\rho = 3T$, assuming the longitudinal scaling behavior $T \sim \tau^{-1/3}$ for the temperature. The result for the equilibration time (which should be considered a lower limit) is

$$\tau_i \geq 0.27 A^{-1/6} \text{ fm/c} , \quad (26)$$

with a corresponding initial temperature at equilibration of

$$T_i \leq 180 A^{1/6} \text{ MeV} . \quad (27)$$

This model could be improved by a more sophisticated matching condition, inserting a kinetic stage between the initial parton distribution and the hydrodynamic regime.

The other model³ is based on the string picture. It uses an Abelian version of the color string between the struck nucleons and employs the Schwinger mechanism to produce $q\bar{q}$ pairs from the electric field in the string. Thermalization is achieved through a collision term parametrized with a constant relaxation time. Requiring boost-invariance of the solution in the direction of the

string, an analytical solution of the Boltzmann equation with a Schwinger source term was obtained, neglecting, however, the acceleration of the produced particles in the electric field. The resulting time dependence of the energy density of the produced particles is shown in Fig. 5, as a function of the ratio τ_0/τ_c where τ_c is the relaxation time from the collision term, and $\tau_0 \sim E_0^{-1/2}$ is the particle formation time which decreases with the initial electric field strength. As shown in Fig. 5a, the energy density initially increases due to particle creation, but then decreases due to longitudinal expansion. It never exceeds ~25% of the initial field energy density. Fig.

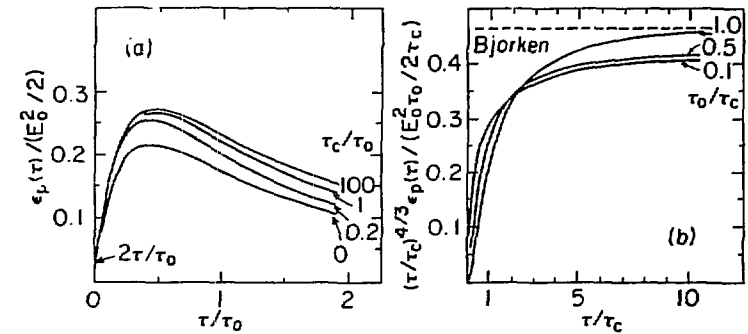


Figure 5. Quark-antiquark energy density in units of the initial electric field energy density (a), and scaled by a factor $(\tau/\tau_c)^{4/3}$ to compare with hydrodynamic behavior (b), computed with the string model. (From Ref. 3)

curve labelled "Bjorken." For longitudinal hydrodynamic expansion the energy density drops as $\tau^{-4/3}$; this behavior is achieved in the model after $\tau \sim 10 \tau_c$, i.e. at times an order of magnitude larger than the collision time. Conversely, extrapolating the energy density back from measured data, using the Bjorken scaling curve, overestimates the energy density at τ_0 , the basic formation time, by a factor 2 to 5. This is an interesting hint as to how one should correct hydrodynamic estimates of the initial conditions (based on measured particle multiplicity densities) for pre-equilibrium phenomena.

This model can be improved by using the non-Abelian generalization of the Schwinger source term²² to describe the color dependence of $q\bar{q}$ pair creation and to include gluon production. Furthermore, acceleration of the particles by the field can be accommodated by including the Vlasov terms in eq. (11). In the constant field of the string, the equations can be simplified by choosing a gauge where the electric field has only $a=3$ and $a=8$ components²². The appro-

appropriate version of the kinetic equations with a Schwinger-type source term is given in my Santa Fe talk²³. They are presently being solved by M. Gyulassy et al.²⁴. A solution neglecting the gluon contribution and the collision term for thermalization was studied by Białas and Czyż²⁵. They found that the acceleration of the particles by the color electric field leads to collective color oscillations which are slowly damped by $q\bar{q}$ pair creation.

5. COLOR OSCILLATIONS AND COLOR EQUILIBRATION

The color kinetic equations (11,12) can be used to determine the color response of a quark-gluon plasma to an external perturbation^{19, 26}. The calculation is easiest for perturbations of a global equilibrium state. One solves the momentum space version of eq. (11) in linear response approximation for the change in the distribution function induced by the perturbation, inserts the result in the expression (16b) for the color currents, and computes from eq. (12) (again in linear approximation and momentum space) the induced color field. The result takes the form

$$\delta A_{\mu}^a(K, \Omega) = R_{\mu\nu}^{ab}(K, \Omega) A_{\nu, \text{ext}}^b(K, \Omega), \quad (28)$$

where $R_{\mu\nu}^{ab}$ is the (causal) color response function. It is diagonal in color, and the Lorentz tensor can be separated into its longitudinal and transverse contributions by using appropriate projection operators¹⁹:

$$R_{\mu\nu}^{ab}(K, \Omega) = \delta^{ab} \left\{ \frac{R_L(K, \Omega)}{k^2 - R_L(K, \Omega)} Q_{\mu\nu} + \frac{R_T(K, \Omega)}{k^2 - R_T(K, \Omega)} P_{\mu\nu} \right\}. \quad (29)$$

Both R_T and R_L depend only on the ratio of Ω/K where Ω and K are the frequency and momentum of the perturbation in the plasma rest frame. For massless quarks they are easily computed analytically, or integrated numerically for massive quarks. The poles in (29) determine the dispersion relation for collective color oscillations. They are shown in Figure 6. Both the longitudinal and transverse modes start at the plasma frequency Ω_p , eq. (25). It turns out that the (massless) quarks dominate the dispersion relation and are responsible for the fact that the longitudinal dispersion relation always stays timelike, and never crosses the line $\Omega = Kc$ as expected from experience with electron-ion plasmas. As a consequence, if the collision term in eq. (11) is omitted, these modes turn out to be undamped; collisionless or Landau damping, a mean field effect and the dominant damping mechanism for longitudinal plasma waves in an electron gas, is kinematically forbidden for timelike momenta and therefore irrelevant for both longitudinal and transverse colored plasma oscillations^{19, 26}.

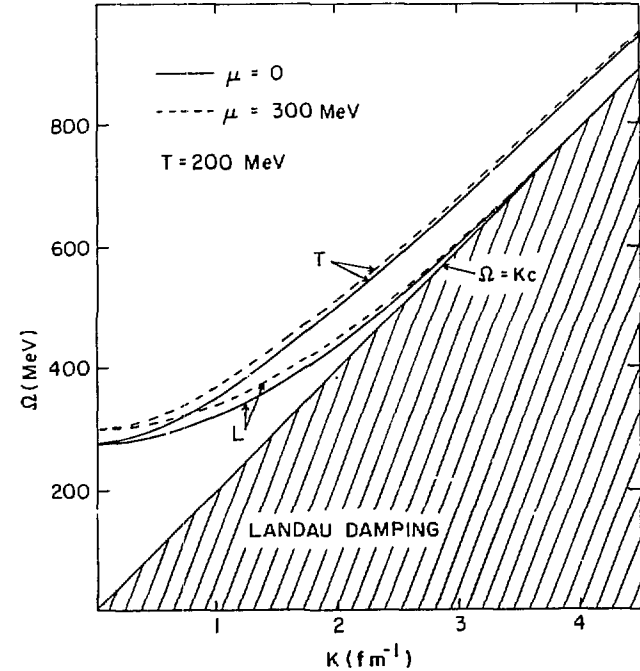


Figure 6. Dispersion relation for longitudinal (L) and transverse (T) colored plasma oscillations. Parameters: $g=2.0$ ($\alpha_s=0.32$); $m_{u,d}=10$ MeV, $m_s=150$ MeV; $T=200$ MeV. The effect of a baryonic chemical potential associated with u and d quarks (dashed vs. solid lines) is minimal. (From Ref. 19)

However, plasmons with timelike momenta can decay into $q\bar{q}$ or gluon pairs. In the electron plasma such decays are usually forbidden because of the large mass threshold, but here the gluons are massless, and even the quark masses can be neglected relative to the plasmon frequency, due to the large temperature. Because of the number of open channels and the Bose enhancement factors, actually gluon pair decay is the dominant origin for an imaginary part to the frequency. It can be computed²⁷ from the discontinuity across the cut of the gauge loop contribution to the 1-loop gluon polarization operator, yielding in Feynman gauge²⁸

$$\Gamma_{L, 2g}(K, \Omega) \equiv \frac{1}{\tau_0(K, R)} \xrightarrow{K \rightarrow 0} -\frac{5g^2}{8\pi} \Omega_p \coth\left(\frac{\Omega}{4T}\right). \quad (30)$$

This agrees in sign, but not in magnitude with a result quoted in Ref. 29 in

the same gauge; however, there the vacuum contribution to the decay rate appears to have been omitted. In eq. (30) we attempted to interpret Γ as an inverse relaxation time²⁷; however, it came out with a negative sign! The ω decay contributes a positive but smaller number so that the net result is still negative. What went wrong?

Let us look at the dissipative part of the color response function as directly computed in finite temperature QCD³⁰; it is related to the gluon polarization operator by changing the Feynman prescription for integration around the poles in the loop propagator to the causal prescription, which keeps only the retarded contributions. On the other hand, its longitudinal part yields the color dielectric function^{31,19}:

$$\text{Re } \epsilon = 1 - \frac{1}{k^2} \text{Re } \pi_L = 1 - \text{Re } R_L ; \quad (31a)$$

$$\text{Im } \epsilon = - \frac{1}{k^2} \tanh \frac{\Omega}{2T} \text{Im } \pi_L = - \text{Im } R_L . \quad (31b)$$

Although the polarization tensor $\pi_{\mu\nu}$ is gauge dependent, the dielectric function ϵ is a physical quantity and should be gauge invariant. The longitudinal color mode shows up as a peak in the imaginary part of ϵ . The width of this peak determines the imaginary part of the collective mode frequency. The sign of $\text{Im } \epsilon$ determines if the mode gets damped or blows up. More generally, for any K and Ω , the sign of $\text{Im } \epsilon(K, \Omega)$ shows whether the system is stable or unstable with respect to a (color) perturbation of frequency Ω and momentum K : if $\text{Im } \epsilon > 0$, the energy contained in the perturbation is absorbed and thermalized by the medium, the perturbation is damped away. This is the case for the electron plasma, as shown in the upper half of Fig. 7.

For $T=0$ the imaginary part of ϵ vanishes for spacelike momenta; at finite temperature the possibility to absorb quanta of the perturbation on the thermally distributed electrons contributes an imaginary part also for spacelike momenta. As indicated, at $T=0$ dissipation of energy from the perturbation into the medium peaks along the longitudinal collective mode.

In the case of a QCD plasma, however, the sign of $\text{Im } \epsilon$ turns negative nearly everywhere^{30,32}. The sign switch at $T=0$ is easily identified; the imaginary part stems from the logarithm in

$$\pi^{\mu\nu}(k^2) = (g^{\mu\nu} - k^\mu k^\nu / k^2) g^2 \frac{2N_f - 5N}{48\pi^2} k^2 \ln(-k^2/M^2) , \quad (32)$$

where M^2 is the UV cutoff. One sees that the same negative sign of the gauge loop relative to the fermion loop that is responsible for asymptotic freedom in QCD also is the culprit for the opposite sign of the imaginary part in QCD

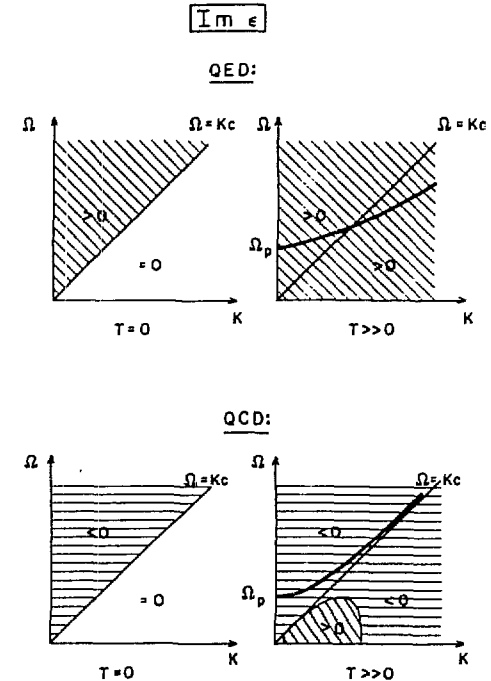


Figure 7. Sign of the imaginary part of the (color) dielectric function in QED and QCD at zero and finite temperature. $\text{Im } \epsilon$ peaks along the longitudinal collective mode as indicated.

compared to QED (where only the term $\sim 2N_f$ is present). Finite temperature effects do not cure this "wrong" sign of $\text{Im } \epsilon$, but rather "enhance" it because now there occurs a strong negative peak along the longitudinal collective mode. Only a small region of spacelike momenta with $K < O(T)$ is stable. (In this region the classical kinetic calculation¹⁹ leading to eq. (29) is reliable, and the sign in Fig. 7 agrees with that calculation, leading to the well-known effect of Landau damping.) Everywhere else the negative sign of $\text{Im } \epsilon$ indicates that the system spontaneously radiates energy³³, i.e. it is intrinsically unstable, not just along the collective mode, but there particularly so. The decay of the longitudinal collective color mode into gluon pairs is the doorway channel towards a new ground state. (Note that a good analogy to this situation is given by a laser, whose unstable initial configuration of inverted population of atomic states is also described by a dielectric function with a negative imaginary part³³.)

The fact that the instability is independent of temperature and does not appear to be affected by color deconfinement and the screening of color electric fields at high T (nor by the smallness of the coupling constant) suggests a problem in the color magnetic sector. Indeed, at $T=0$ it is known that the perturbative vacuum is unstable against spontaneously developing a constant color magnetic field³⁴. Although the minimum in the effective potential at a nonvanishing value for \vec{B} evaporates at large temperature³⁵, this does not imply restoration of the perturbative vacuum: the effective potential in a magnetic background field has an imaginary part due to unstable modes, and these modes are not stabilized at finite T ³⁷. At $T=0$ they were shown to lead to a complicated structure of electric vortex lines or magnetic flux tubes in the QCD vacuum³⁶, yielding the so-called "spaghetti vacuum" of the Copenhagen group. This spaghetti vacuum was argued to have a lower energy than the perturbative one even at finite temperature³⁷.

I suggest that the same unstable modes are responsible for our negative sign of the dielectric function in QCD: they correspond to imaginary energy eigenvalues³⁶ which implies that the QCD Hamiltonian is not Hermitian in the Fock space which includes the perturbative vacuum. As a consequence, the Lehmann representation¹⁹ for $\text{Im } \epsilon$ is not required to be positive definite since it sums over all states including the unstable vacuum state: Matrix elements

connecting to this state do not fulfill the relationship $M_{0n} = M_{n0}^*$, explaining how $\text{Im } \epsilon \sim \sum_{n,m} \dots \langle n|M|m\rangle \langle m|M|n\rangle \neq \sum_{n,m} \dots |\langle n|M|m\rangle|^2$ can become negative in QCD.

According to this analysis, the wrong sign in the damping rate for collective color oscillations and in the relaxation time for the collision term responsible for color conduction is due to an expansion around the wrong vacuum state. The quark-gluon plasma never attempts to reach a locally color neutral state of thermally distributed quarks and gluons in an otherwise empty vacuum. Rather, the vacuum itself has local color structure³⁸, even at arbitrarily high temperature. As a consequence, the physical degrees of freedom in the plasma will not be free quarks and gluons, but "quasiquarks" and "quasigluons" which are dressed according to the interaction of the free particles with the structures vacuum. This explains the so far unsurmounted difficulties with perturbation theory in finite temperature QCD³⁹, which can only be expected to be cured once the correct spectrum of quasiparticles has been found. Then the kinetic theory should be reformulated on the basis of these effective degrees of freedom, if we ever hope to use it for a description of the approach to local thermal equilibrium.

6. SUMMARY

The first steps towards a non-equilibrium description of the quark-gluon plasma dynamics have been made. We have learned how to adapt kinetic theory to a relativistic system with non-Abelian interactions, in particular how to treat the color degrees of freedom. The connection between a pre-equilibrium description at an early stage and hydrodynamics at later times has been thoroughly investigated and, given some typical relaxation times, transport corrections to ideal hydrodynamics have been computed. A major difficulty is still the definition of initial conditions for the phase-space distribution function appropriate for relativistic heavy-ion collisions. Also the quantum theoretical foundation of kinetic plasma theory, in particular of the gluon sector, needs much more work. First applications of the classical kinetic framework to a near-equilibrium quark-gluon plasma yielded as useful results the spectrum of collective color modes in such a plasma. However, these modes turned out to be unstable. This instability was argued to be due to a basic problem with our conventional picture of the quark-gluon plasma as a thermal distribution of weakly interacting particles in a perturbative vacuum: this state appears to be unstable against developing local color structures.

On the one hand, this looks like an unfortunate setback, because we would need to first compute the properties of the new, stable vacuum and its quasi-particle spectrum, before kinetic theory can be reformulated in a sensible way that is free from these instabilities. On the other hand, difficulties with perturbation theory have indicated a need for this before, and that we stumble at this point may be a blessing in disguise: we will be prompted to have a very careful look at many existing calculations of plasma signatures (e.g. lepton pair spectra, direct photons, etc.) which are based on this oversimplified picture. Also, we have to watch the results from lattice Monte Carlo calculations with new eyes, in particular when we try to interpret the apparent T^4 -behavior of the energy density seen above the deconfinement transition: if not free quarks and gluons, what else can generate such a behavior? Can we recognize color structures in the QCD vacuum below and above the transition from the output of these calculations? How do they change with T and μ ?

We see that as we grope our way towards describing the pre-equilibrium state of quark matter in heavy-ion collision, the equilibrium state itself has become the focus of our scrutiny again. Obviously, interesting discoveries lie in front of us!

ACKNOWLEDGEMENTS

Interesting discussions with G. Baym, G. Brown, H. Hansson, K. Kajantie, L. McLerran, P. Siemens, and L. van Hove during and after the conference helped to sharpen the arguments presented in section 5 (although several of these colleagues may still not agree with them). I thank all of them for their lively interest in the matter.

REFERENCES

- 1) H. von Gersdorff, L. McLerran, M. Kataja, and P.V. Ruuskanen, Fermilab preprint 86/13-T.
- 2) K. Kajantie, M. Kataja, L. McLerran, and P.V. Ruuskanen, Helsinki preprint HU-TFT-86-6.
- 3) K. Kajantie and T. Matsui, Phys. Lett. 164B (1985) 373.
- 4) U. Heinz, P.R. Subramanian, H. Stöcker, and W. Greiner, J. Phys. G (1986), in print.
- 5) P. Koch, B. Müller, and J. Rafelski, Phys. Rep. (1986), in print; see also B. Müller's talk at this conference.
- 6) H. Stöcker and W. Greiner, Phys. Rep. (1986), in print.
- 7) J. Aichelin, in: Local Equilibrium in Strong Interaction Physics II, Proceedings of the Workshop in Santa Fe, New Mexico, April 8-12, 1986 (Scientific Publishing Co., Singapore, 1986).
- 8) L.W. Nordheim, Proc. Roy. Soc. London A119 (1928) 689.
- 9) Such a calculation is presently set up by the Helsinki group (K. Kajantie, private communication).
- 10) S.K. Wong, Nuovo Cimento A65 (1970) 689.
- 11) U. Heinz, Ann. Phys. 161 (1985) 48.
- 12) R. Balescu, Equilibrium and Non-Equilibrium Statistical Mechanics, chpt. 3.6 (Wiley, New York, 1975).
- 13) H.-Th. Elze, M. Gyulassy, and D. Vasak, Nucl. Phys. B (1986), in print.
- 14) U. Heinz, Phys. Rev. Lett. 53 (1983) 351.
- 15) M. Ploszajczak and M.J. Rhoades-Brown, Phys. Rev. Lett. 55 (1985) 147, and Phys. Rev. D, in print.
- 16) P. Danielewicz and M. Gyulassy, Phys. Rev. D31 (1985) 53.
- 17) A. Hosoya and K. Kajantie, Nucl. Phys. B250 (1985) 666.
- 18) S. Gavin, Nucl. Phys. A435 (1985) 826.
- 19) U. Heinz, Ann. Phys. 168 (1986).
- 20) R. Hwa, see Ref. 7.
- 21) R. Hwa and K. Kajantie, Phys. Rev. Lett. 56 (1986) 696.
- 22) M. Gyulassy and A. Iwazaki, Phys. Lett. 165B (1985) 157.
- 23) U. Heinz, see Ref. 7.
- 24) M. Gyulassy, private communication.
- 25) A. Bialas and W. Czyz, raport IFJ 1307/PH, to be published in Acta Physica Polonica B (1986).
- 26) U. Heinz and P. Siemens, Phys. Lett. 158B (1985) 11.
- 27) H.A. Weldon, Phys. Rev. D28 (1983) 2007.
- 28) U. Heinz and H.A. Weldon, unpublished.
- 29) K. Kajantie and J. Kapusta, Ann. Phys. 160 (1985) 477.
- 30) J.A. Lopez, J.C. Parikh, and P.J. Siemens, Instability of the QCD Plasma, Texas A&M preprint 1986.
- 31) H.A. Weldon, Phys. Rev. D26 (1982) 1394.
- 32) Ref. 30 has a slightly different arrangement of signs in QCD at finite T than shown in the lower right diagram of Fig. 7. Figure 7 is based on my own recalculation of $\text{Im } \epsilon$ in finite temperature QCD, using the same methods as Ref. 30.
- 33) J.D. Jackson, Classical Electrodynamics, chpt. 7.5 (Wiley, New York, 1975).
- 34) G.K. Savvidy, Phys. Lett. 71B (1977) 133; N.K. Nielsen and P. Olesen, Nucl. Phys. B144 (1978) 376;
- 35) B. Müller and J. Rafelski, Phys. Lett. 101B (1981) 111; J. Kapusta, Nucl. Phys. B190 (1981) 425.
- 36) N.K. Nielsen and P. Olesen, Phys. Lett. 79B (1978) 304; H.B. Nielsen and P. Olesen, Nucl. Phys. B160 (1979) 380; J. Ambjorn and P. Olesen, Nucl. Phys. B170 (1980) 60.
- 37) W. Dittrich and V. Schanbacher, Phys. Lett. 100B (1981) 415; A. Cabo, O. K. Kalashnikov, and A. E. Shabad, Nucl. Phys. B185 (1981) 473; E. Elizalde and J. Soto, Phys. Rev. D (1986), in print
- 38) see J. Polonyi's talk at this conference.
- 39) see B. Svetitski's talk at this conference.